FLEXURAL DUCTILITY OF FULL-SCALE RC BRIDGE COLUMNS SUBJECTED TO CYCLIC LOADING

Jun-ichi Hoshikuma[1], Shigeki Unjoh[2], Kazuhiro Nagaya[3]

1 Senior Research Engineer, Earthquake Eng. Div., Public Works Research Institute
2 Head, Earthquake Eng. Div., Public Works Research Institute
3 International Division for Infrastructure, Policy Bureau, Ministry of Land, Infrastructure and Transport

Keywords: size effect, ductility, reinforced concrete columns, full-scale test

1 INTRODUCTION

Many researchers previously proposed the ductility assessment procedures for flexural reinforced concrete columns subjected to seismic action[1),2),3),4)]. These are established based on mainly experimental results and statistical studies for their data. It should be suggested that such empirical approaches have a limit for application. Some existing ductility assessment procedures note the applicable limits in terms of the flexure-shear strength ratio, longitudinal steel ratio, transverse steel ratio, axial force ratio, aspect ratio, etc. However, the limit of cross sectional size is unclear in the previous proposals, and the size effect on the inelastic behavior of reinforced concrete columns is also unknown.

There is an important research work regarding the size effect reported by Stone and Cheok[5)]. They conducted a series of cyclic loading test for full-scale circular columns (diameter= 1524mm) and their well-scaled replica model, to determine the size effect on inelastic behavior of reinforced concrete columns subjected to seismic force. A comparison of test results between full-scale and replica columns showed that the size effect on failure mode, energy absorption property and ductility capacity was less significant. It is an interesting finding that the size effect does not appear when reinforcement details including bar diameter and vertical hoop spacing are scaled down precisely based on a scale factor.

Though there is a research on the size effect on flexural ductility as described above, the size of cross section in reinforced concrete columns constructed in Japan is still larger than Stone and Cheok's columns. Furthermore not only circular but rectangular cross section is often designed in Japanese bridge columns. Since the rectangular section is less effective confinement than circular section, the size effect has been controversial issue for particularly rectangular section.

This research program was initiated with motivation to investigate the size effect on inelastic behavior of reinforced concrete columns with big square cross section that never tested. Full-scale columns with 2400mm square section and 9600mm height were loaded until the columns were completely failed, and inelastic behavior of the plastic hinge region was studied. Furthermore, a 1/4-scale replica model was also tested for comparison with the full-scale column behavior, and the size effect was discussed based on test results.

2 CYCLIC LOADING TEST PROGRAM

2.1 Test Units Details

Two full-scale columns (called herein L1 and L2) and one replica column (called herein S1) were tested in the program, and their structural details are shown in Fig. 1 and Fig. 2. The unit L2 is a reference column and the unit S1 is a 1/4-scale replica model of the L2. The unit L1 is a model with the same size and longitudinal steel ratio as the L2 but the transverse steel ratio reduced.

The full-scale columns have 2.4m square cross section with column height of 9.6m, resulting in the aspect ratio of 4.0. The column section has 72 D35 (diameter=35mm) longitudinal bars in one layer distributed evenly with a constant cover of 102mm. The longitudinal steel ratio to net area of the concrete is 1.2%. The hoop bar was fabricated with two D19 (diameter=19mm) L-shaped reinforcements and placed with 300mm (L1) or 150mm (L2) vertical spacing. Each hoop bar has 135-degree hooks with 190mm leg at both end edges. Furthermore, for the unit L2, cross ties were placed at each hoop level as depicted in Fig. 1(b). Each cross tie has the 180-degree hook with 250mm

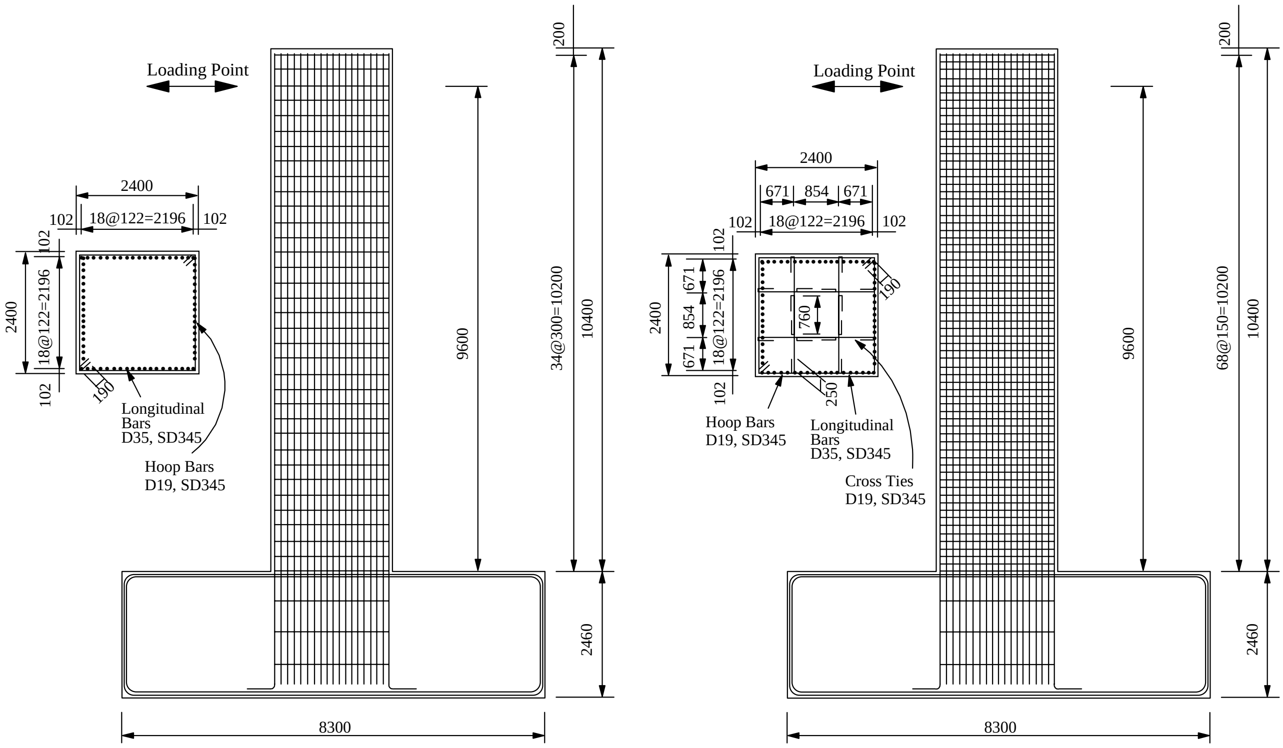

(a) Unit L1 (b) Unit L2

Fig. 1 Structural Details of Full-scale Columns

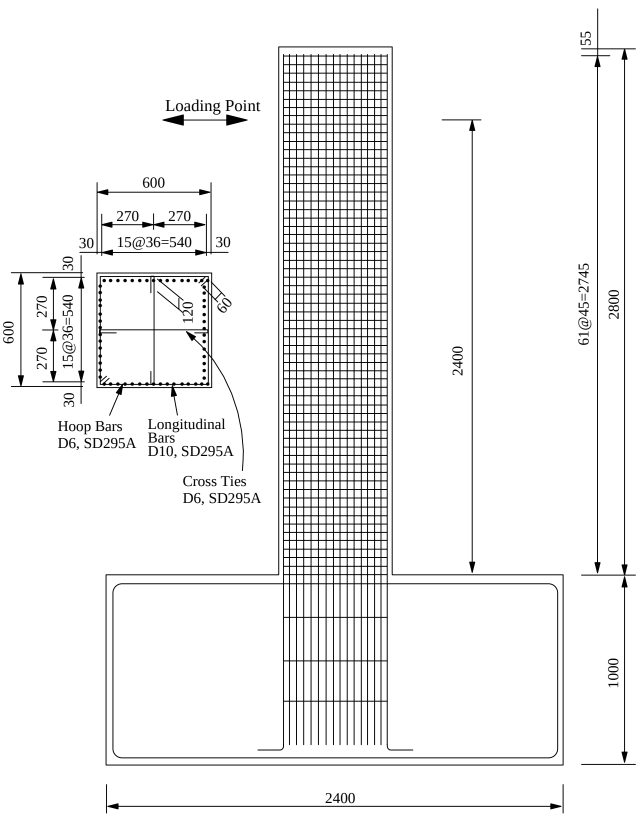

Fig. 2 Structural Details of Replica Model

Table 1 Material Properties

(a) Concrete Strength

Unit	Column (N/mm^2)	Footing (N/mm^2)
L1	33.5	37.3
L2	32.6	38.0
S1	39.0	39.0

(b) Reinforcement

Unit	Steel Bars	Dia.	Young's Modulus (N/mm^2)	Yield Strength (N/mm^2)	Tensile Strength (N/mm^2)
L1 L2	Long.	D35	1.77×10^5	424	639
	Hoop	D19	1.72×10^5	344	528
S1	Long.	D10	1.78×10^5	395	565
	Hoop	D6	1.85×10^5	389	534

Table 2 Comparisons of Structural Details between L2 and S1

	L2	S1	L2 / S1 (Ideal Value)
Dimension of Section (mm)	2400 x 2400	600 x 600	4.0 (4.0)
Column Shear Span (mm)	9600	2400	4.0 (4.0)
Aspect Ratio	4.0	4.0	1.0 (1.0)
Diameter of Long. Bar (mm)	35	10	3.5 (4.0)
Long. Bar Spacing (mm)	122	36	3.39 (4.0)
Long. Steel Ratio	0.012	0.012	1.0 (1.0)
Diameter of Lateral Bar (mm)	19	6	3.17 (4.0)
Lateral Bar Spacing (mm)	150	45	3.33 (4.0)
Effective Length of Confined Concrete (mm)	854	270	3.16 (4.0)
Volumetric Lateral Steel Ratio	0.0089	0.0104	0.86 (1.0)
Max. Aggregate Size (mm)	20	20	1.0 (4.0)

leg at end edges and the hoop bar was hooked by the cross tie. Due to complicated construction of the cross ties with hooks, cross ties were spliced in the core with 760mm lap length.

On the other hand, the unit S1 was designed based on structural details of the unit L2. Sixty reinforcements of D10 (diameter=10mm) were placed for longitudinal bars in one layer distributed evenly with a constant cover of 30mm. It should be suggested that 8.75mm diameter bar is the most appropriate for longitudinal bar in terms of the similitude relationships since D35 bars were used in the full-scale columns. However, such standardized reinforcement is unavailable. Therefore, the D10 bars were selected from available reinforcement. Consequently, the horizontal spacing of the longitudinal bar was adjusted from the similitude value, to equalize the longitudinal steel ratio. The hoop bar consisted of the D6 deformed bars with 135-degree hooks embedded into the core by 120mm leg. Cross ties was arranged as shown in Fig. 2 and the ends of these cross ties were hooked to hoop bar with the 180-degree hooks. Since it was also impossible to scale down the hoop diameter precisely due to a limitation of available reinforcement, the center-to-center spacing of the hoop bars were adjusted so as to approximate the transverse steel ratio of the unit L2.

Material properties of concrete and reinforcement used for the test units are listed in Table 1.

2.2 Comparison of Structural Details between Full-scale and Replica Column

Structural details comparison between the unit L2 and S1 was summarized in Table 2, where the effective length of confined core was defined as the maximum horizontal spacing of cross ties, and the volumetric ratio of lateral reinforcement was defined as Eq. (1).

$$\rho_s = \frac{4A_s}{s \cdot d} \qquad (1)$$

where, ρ_s : volumetric ratio of transverse reinforcement to the confined core
A_s : area of transverse reinforcement
s : vertical spacing of transverse reinforcement
d : effective length of confined core

Table 2 shows that reinforcement arrangement of the replica model S1 was designed as well-scaled to the full-scale L2 column as possible. However, it should be noted that the replica model was not perfectly-scaled-down column.

2.3 Loading Setup and Loading Pattern

Photo 1 shows a set-up of the loading system for the full-scale column tests. Lateral load was applied using two 3000kN large-stroke hydraulic actuators. Unfortunately a vertical load was not applied in this project because it was very difficult to give the vertical load in the loading system we used for lack of capacity of the reaction floor. However, specific objective of the research is to examine the size effect on the inelastic behavior of the flexural reinforced concrete columns, and thus even though the vertical load was not applied, conclusions of the size effect derived from the experimental discussion could be generalized.

The unit S1 was loaded as shown in Photo 2, where the column base was fixed to the reaction wall. The vertical load was not applied so as to create the same condition with the full-scale column tests. The columns were loaded quasi-statically and subjected to cycles of force reversals under the force control until yielding of the extreme longitudinal reinforcement. A yield displacement $1\delta_y$ was determined here as a displacement at the loading point of column when the extreme longitudinal bars yielded at the base section. Based on measured strain of the extreme longitudinal bars, the yield displacement was defined as 50mm for the full-scale columns and 10mm for the replica model. Subsequently, the lateral displacement was applied with stepwise increasing amplitude ($\pm 1\delta_y$, $\pm 2\delta_y$, $\pm 3\delta_y$, ・・・・) under the displacement control. The cyclic number in each loading step was three.

3 INELASTIC COLUMN BEHAVIOR

3.1 Lateral Strength and Drift Hysteresis Loops

Experimental lateral load-drift responses of the test units were shown in Fig. 3. Regarding the unit L1, the lateral load-drift loop exhibits stable response up to the first cycle of $4\delta_y$ (drift ratio=0.021). In the second cycle of $4\delta_y$, buckling of the longitudinal bars was observed following cover concrete spalling and hoop bars swelled out. The lateral load-drift loop became unstable from this loading cycle. The lateral load-drift loop of the unit L2 is stable up to the first cycle of $5\delta_y$ (drift ratio=0.026) and the pinching effect appears after the second loading cycle resulting from buckling of longitudinal bars. This observation is similar to the unit L1.

On the other hand, for the unit S1, the lateral force kept peak strength with stable response curve up to the second cycle of $6\delta_y$ (drift ratio=0.025) loading. Spalling of cover concrete following longitudinal bar buckling was observed in the third cycle of $6\delta_y$. It is noted that the pinching of the hysteresis loops arise from buckling of longitudinal bars and spalling of cover concrete in both full-scale and replica models.

3.2 Lateral Strength and Ductility

Fig. 4 compares the contour of the lateral force and drift hysteresis loops between the unit L2 and S1. The lateral force measured for the unit S1 was modified based on Eq. (2) so as to make a relative comparison the test results.

$$P_{se} = P_s \, s_\ell^{\,2} \qquad (2)$$

where, P_{se} : modified lateral force of unit S1
P_s : lateral force measured for unit S1
s_e : scale factor (=4.0)

Fig. 4 indicated that the contours of the unit L2 and S1 exhibited similar response. The maximum lateral force of the unit L2 was slightly larger than that of the unit S1. This difference arises from the difference of yield strength of longitudinal reinforcement between both units as listed in Table 1. Though the longitudinal reinforcement ratio was equivalent as 0.012, the yield strength of longitudinal reinforcement in the unit L2 was 7% larger than that in the unit S1.

Photo 1 Full-scale Column Test

Photo 2 Replica Model Test

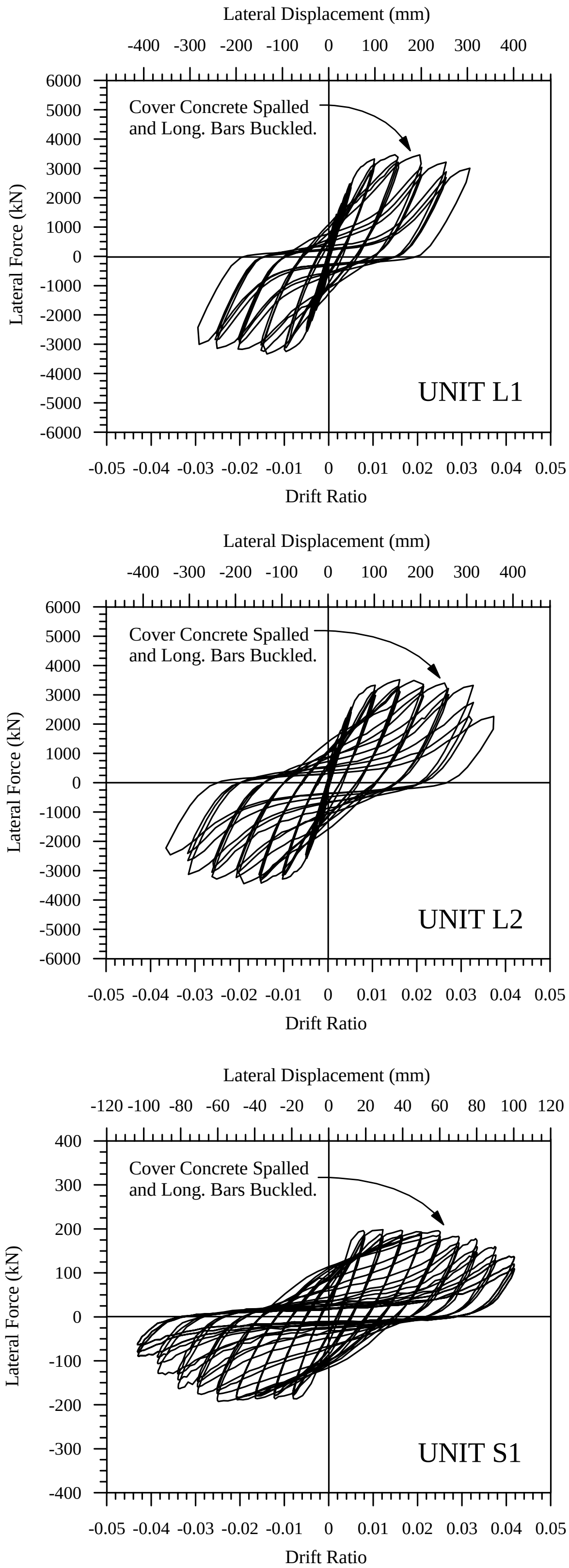

Fig. 3 Experimental Hysteresis Loops of Test Units

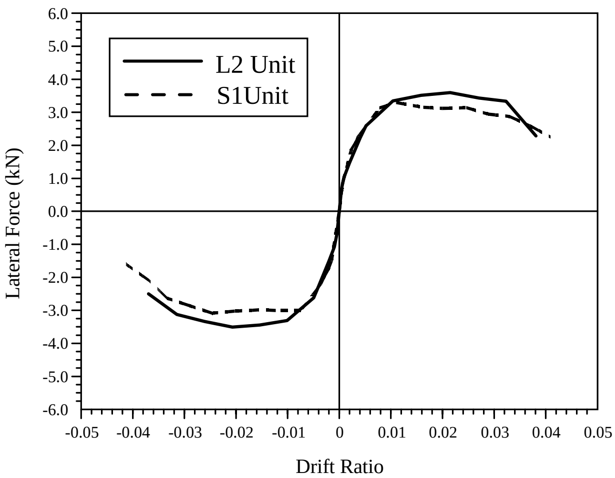

Fig. 4 Contour of Hysteresis Loops

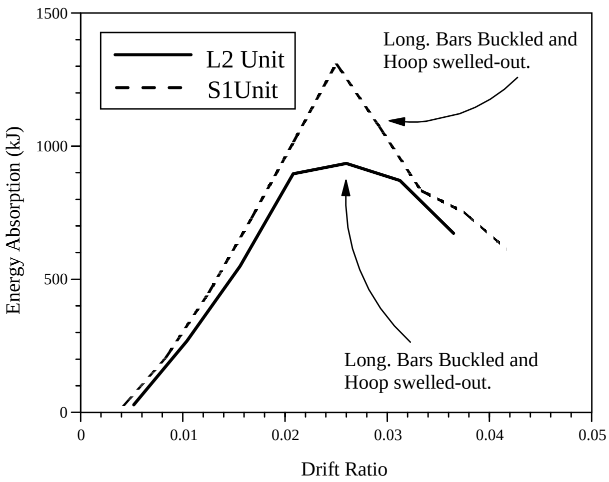

Fig. 5 Comparison of Energy Absorption

3.3 Inelastic Energy Capacity

Energy absorption capacity is one of the effective indexes for measuring overall column performance subjected to cyclic action. The amount of energy absorption was determined by the area bounded by the load-displacement hysteresis loops. Fig. 5 shows the amount of energy absorption in each ductility level calculated for the units L2 and S1. Inelastic energy absorption in the unit S1 was modified through Eq. (3), so that inelastic energy absorption can be compared relatively between two units.

$$\Delta W_{Se} = \Delta W_S \, s_\ell^{\,3} \qquad (3)$$

where, ΔW_{Se} : modified inelastic energy absorption of unit S1
ΔW_S : inelastic energy absorption of unit S1 calculated for the first cycle of each ductility level
s_ℓ : scale factor (=4.0)

It is noted that the amount of inelastic energy of the units L2 and S1 are similar up to 0.02 of drift ratio, and that the inelastic energy absorption during the first loading cycle reaches the peak when the longitudinal bars buckle and consequently hoop bars swell-out. However, in the range of 0.02 to 0.03 of drift ratio, the amount of energy absorption in S1 was larger than that in the full-scale column.

4 SIZE EFFECT ON PLASTIC CURVATURE PROFILES

Fig. 6 shows the curvature profiles measured for test units during inelastic loading steps. The regions where the longitudinal reinforcement yielded, and where cover concrete was spalled-off resulting from buckling of longitudinal reinforcement, were indicated in the figure, respectively. Curvatures were measured up to the height of 3640mm for the full-scale columns and 937mm for the replica model. Column base rotation was excluded from curvature measured at the section near column bottom, because it arises from the bond slip of longitudinal reinforcement in the footing and this effect should be distinguished from column curvature response.

Fig.7 compares the curvature profiles measured when cover concrete began to spall-off between the units of L2 and S1. Column height and the measured curvatures for the S1 unit were modified based on similitude relationships for relative comparison with the L2. It can be noted that the both units exhibit similar curvature profiles when the columns suffer from the damage as cover concrete spall resulting from buckling of the longitudinal reinforcement. This fact indicates that the size effect on the curvature profiles around the plastic hinge region is not so significant as long as structural details of a replica model is well-scaled down based on a prototype column.

5 SIZE EFFECT ON BASE ROTATION DUE TO BOND SLIP OF DEVELOPED BARS

Lateral displacement measured at the loading point consists of deflection due to flexure/shear and base rotation resulting from bond slip of longitudinal bars in the footing. It has been suggested that an

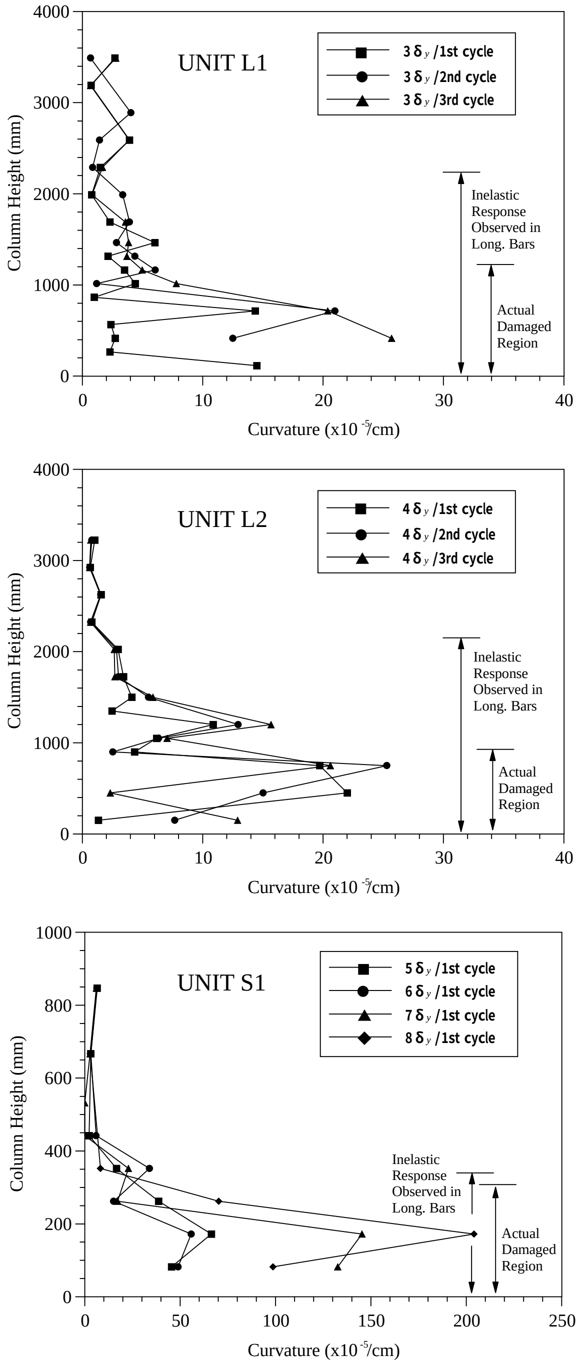

Fig. 6 Measured Curvature Profiles

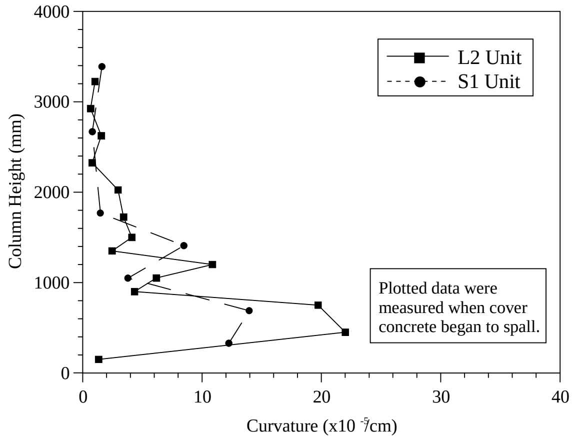

Fig. 7 Comparison of Curvature Profiles between L2 and S1 Units

amount of the longitudinal bar extension due to slippage may be one of factors of the size effect and the lateral displacement resulting from bond slip of longitudinal bars should not be expected in the ductility evaluation of the full-scale reinforced concrete columns.

Because of difficulty in measuring the longitudinal bar extension directly, the column base rotation was measured through two LVDTs amounted each on the flange faces at the column base. The LVDT brackets were connected to aluminum angles that were supported by thread rods anchored to either side of the column core. The reference length for LVDTs was determined as short as possible not to include curvature component at near column base. This measuring system was effective until cover concrete began to spall-off.

In this study, measured lateral displacements were divided into flexure/ shear component and bond slip component. Then lateral displacement at loading point due to bond slip of developed bars was estimated through Eq. (4).

$$\delta_\theta = \theta \times L \qquad (4)$$

where, δ_θ : lateral displacement at loading point due to bond slip of developed bars
θ : measured base rotation
L : column shear span

Fig. 8 compares the ratio of δ_θ to the measured total lateral displacement δ between the units L2 and S1. The value of δ_θ / δ would be affected by longitudinal bar diameter, bond strength, deterioration in flexural stiffness of the critical section due to inelastic cyclic loading and longitudinal tensile strain profiles of the developed bars in footing. For the unit L2, the value of δ_θ / δ is around 0.2 but it slightly increases with increasing the drift ratio of the column. On the other hand, the value of δ_θ / δ in the unit S1 was 0.15 to 0.35, which exhibited larger change than the result of the unit L2. It increases up to 0.012 of drift ratio, and subsequently decreases as the drift ratio increases. However, it should be noted that the lateral displacement due to bond slip of longitudinal bars was observed clearly in the full-scale column as well as the replica model. Furthermore, with viewing overall behavior shown in Fig. 8, the value of δ_θ / δ is roughly equivalent to that for the replica model.

6 CONCULUSIONS

This paper reports the cyclic loading test results for the full-scale square reinforced concrete bridge columns and their replica model. The size effect on inelastic behavior of reinforced concrete columns was discussed through a comparison of test data.

The contour of lateral force and drift hysteresis loop for the full-scale column was relatively similar to that for its replica model. The amount of inelastic energy for the full-scale column also coincided with that for the replica model up to 0.02 of drift ratio. Curvature profiles measured when cover concrete spalled corresponded well for both columns. Furthermore, the base rotation resulting from bond slip of the longitudinal bars was not affected significantly by the size of column section. Therefore, it could be concluded that the size effect on the inelastic ductile behavior of reinforced concrete bridge columns would not be significant as long as we tested.

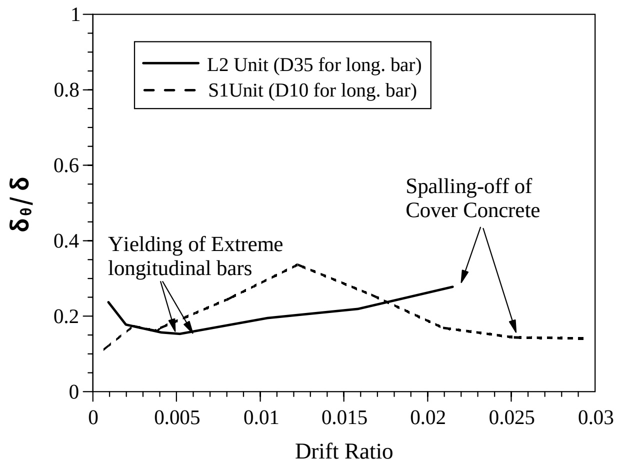

Fig. 8 Lateral Displacement due to Bond Slip of Longitudinal Bars

It should be, however, noted that above conclusions derive from the cyclic loading test for the replica model designed with paying careful attention to the scale factor. Stone and Cheok's test results also indicated that the size effect did not appear clearly on the inelastic behavior of reinforced concrete columns. This would be because the replica model they designed was scaled down very precisely. For example, diameter of longitudinal reinforcement affects bond slip behavior in the footing and the plastic hinge length. Vertical hoop spacing affects the buckling length of the longitudinal reinforcement and thus the plastic hinge length. Therefore, it is important in designing of replica model to determine not only the longitudinal/transverse reinforcement ratio but also the diameter of longitudinal reinforcement and vertical hoop spacing based on the scale factor. These details should be scaled down as precisely as possible, otherwise the size effect would develop in the inelastic behavior and ductility capacity of reinforced concrete columns.

ACKNOWLEDGMENTS

This research presented in this paper was one of products of the joint research program on the size effect on the seismic behavior of reinforced concrete bridge columns. This program has been conducted by the Public Works Research Institute, Japan Highway Public Corporation, Metropolitan Expressway Public Corporation and Hanshin Expressway Public Corporation. The authors wish to appreciate all participants in the joint research program for their work.

REFERENCES

1) Priestley, M.J.N., Seible, F. and Calvi, G.M. : Seismic Design and Retrofit of Bridges, Wiley-Interscience, 1996.
2) Priestley, M.J.N. and Park, R. : Strength and Ductility of Reinforced Concrete Bridge Columns Under Seismic Loading, ACI Structural Journal, Vol. 84, No.1, pp.61-76, Jan.-Feb. 1987.
3) Hoshikuma, J., Kawashima, K. and Unjoh, S. : Ductility Evaluation of Reinforced Concrete Bridge Columns, Second Italy-Japan Workshop on Seismic Design and Retrofit of Bridges, Feb., 1997.
4) Japan Society of Civil Engineering : Standard Specifications of Concrete Structures, 1996. (in Japanese)
5) Stone, W.C. and Cheok, G.S. : Inelastic Behavior of Full-Scale Bridge Columns Subjected to Cyclic Loading, NIST Building Science Series 166, National Institute of Standards and Technology, U.S. Department of Commerce, Jan. 1989.